

Impact of loss mechanisms on performances of perovskite solar cells

Shurong Wang^{a,1}, Yinsheng Peng^{b,*1}, Long Li^b, Zhineng Zhou^a, Zuming Liu^a, Shouli Zhou^b, Minghai Yao^b

^a Key Laboratory of Rural Energy Engineering in Yunnan Province, Yunnan Normal University, Kunming, 650500, PR China

^b College of Information and Engineering, Zhejiang University of Technology, Hangzhou, 310023, PR China



ARTICLE INFO

Keywords:

Perovskite solar cell
Loss mechanism
Nonradiative recombination
Solar cell performance
Power conversion efficiency

ABSTRACT

With the progress in device research, the power conversion efficiency (*PCE*) of perovskite solar cells is continuously improving and is approaching its theoretical limit. Nonetheless, it is still below the efficiency limit predicted by Shockley-Queisser owing to the presence of loss mechanisms. In this paper, we comprehensively analyze the loss factors limiting performance of devices utilizing an equivalent circuit model and identify the dominant loss mechanisms. The results demonstrate that Shockley-Read-Hall recombination and series resistance is the most important two of factors limiting the performance of perovskite solar cell. Shunt resistance and surface recombination plays slight roles in *PCE* when they are greater than $10^4 \Omega \cdot \text{cm}^2$ and less than 10^4cm/s , respectively. Auger recombination has almost no impact on the device performance.

1. Introduction

Organic-inorganic $\text{CH}_3\text{NH}_3\text{PbI}_3$ perovskite solar cells have received continuous attention in the photovoltaic field due to their advantages such as high carrier mobility [1], long carriers diffusion length [2–5] and direct band gap [6–9] and so on. In addition, Perovskite is one kind of very economical material and can be processed cost-effectively utilizing easy methods such as solution or evaporation methods and so on [10].

The highest power conversion efficiency (*PCE*) of thin-film perovskite solar cells has been certified and reached an impressive efficiency closed to 26% [11]. Despite this high efficiency, it is currently less than the limiting efficiency of 31% predicted theoretically by Shockley-Queisser (SQ) [12]. Therefore, it is urgently necessary to quantify the key loss mechanisms limiting the *PCE* of perovskite solar cells. In this paper, our goal is to simulate numerically the fundamental loss processes that limiting perovskite solar cell performance by utilizing an equivalent circuit model [13] combined with framework of the Shockley-Queisser theory [14] as well as principle of detailed balance [15], thereby identify the key loss mechanisms.

Although the impact of loss mechanisms on performance of thin film GaAs solar cells has been discussed by Xufeng Wang et al. in this literature [16], the impact on that of perovskite solar cells is rarely reported. Recently, the efficiency gains of perovskite solar cells are correlated with

increasing open-circuit voltage (V_{oc}) by enhancing the photon recycling effect [17,18], which can be explained as follows. The photons emitted by radiative recombination have possibility of being reabsorbed within the active layers before escaping the cell. In the steady-state situation, the carrier density is scaled up by $np = n_i^2 \exp(\mu/kT)$, which is determined by the internal chemical potential μ , thus V_{oc} increases through $\mu = qV_{oc}$ [19–22]. However, recent literatures [23–25] have shown that low photoluminescence quantum efficiency (PLQE) limits the degree of photon recycling observed in perovskite films because of its high non-radiative recombination rate of approximate $10^6 \sim 10^9 \text{s}^{-1}$, accompanied by a trap state density of $10^{15} \sim 10^{17} \text{cm}^{-3}$ [26–28]. On the other hand, several reports have observed the phenomenon that an emission spectra redshift as a function of time due to photon recycling effect in thick perovskite single crystals by utilizing time-resolved photoluminescence spectroscopy, which is due to low bulk defect densities. However, the high surface recombination velocity of 5800 cm/s results in excess carrier rapid recombination, which decreases the photon recycling effects [29–33]. Therefore, it is necessary to consider that the impact of active layer thickness and surface recombination besides bulk recombination on the performance of perovskite solar cells.

At present, it is usually believed that the non-radiative recombination in solar cells mainly include bulk Shockley-Read-Hall (SRH) recombination, bulk Auger recombination and surface recombination.

* Corresponding author.

E-mail address: yspeng@zjut.edu.cn (Y. Peng).

¹ Shurong Wang and Yinsheng Peng have equal contributions to this paper and are tied as the first authors.

The bulk SRH recombination is primarily related to the defects and impurities in the active layer, while the surface recombination is primarily related to the surface defects. Therefore, the impact of non-radiative mechanism on the characteristics of perovskite solar cells need to analyze and quantify. Although several works have discussed the effects of radiative recombination, SRH and Auger recombination on perovskite solar cells [34–37]. But these literatures do not involve the impact of surface recombination and ohmic resistance on the properties of perovskite solar cells. In this paper, we explore the practical aspects of perovskite solar cells, comprehensively considering photon recycling, ohmic losses, radiative and nonradiative recombination losses, and describes their impact on the properties of practical perovskite solar cells, thereby identify the dominant loss mechanisms.

1.1. Model and formulas

In this paper, an equivalent circuit model of a practical perovskite solar cell is shown in Fig. 1, which comprehensively considers radiative and nonradiative loss as well as ohmic loss.

The current-voltage equations are described as

$$J(V) = J_{ph} - J_e - J_{nr} - J_{sh} \quad (1)$$

$$J_{nr} = J_{surf} + J_{bulk} \quad (2)$$

$$J_{bulk} = J_{srh} + J_{aug} \quad (3)$$

where the J_{ph} : photogenerated current density

J_e : external radiative current density

J_{nr} : non-radiative recombination current density

J_{surf} : surface recombination current density

J_{srh} : Shockley-Read-Hall recombination current density

J_{sh} : shunt resistance current density (leakage current)

The photogenerated current density can be obtained by equation (4) as below.

$$J_{ph} = \frac{q}{hc} \int_{\lambda_{min}}^{\lambda_{max}} \lambda a(\lambda) I(\lambda) d\lambda \quad (4)$$

where c is the speed of light in free space, $I(\lambda)$ is the global AM1.5G spectrum of sun ($W \cdot m^{-2} \cdot nm^{-1}$), q is the elementary charge, $a(\lambda)$ is photon absorptivity corresponding to wavelength of λ , λ_{min} , λ_{max} are 310 nm and 775 nm, respectively.

In this paper, for simplicity, an ideal solar cell model is utilized with zero-reflectivity textured front surface and unity reflectivity at the rear side. The absorptivity of a textured cell could be derived from Refs. [38, 39]:

$$a(\lambda) = \frac{4n^2\alpha L}{4n^2\alpha L + 1} \quad (5)$$

where α and n are wavelength-dependent absorption coefficient and refractive index data for $CH_3NH_3PbI_3$ [40], respectively, L is the thickness of active layer.

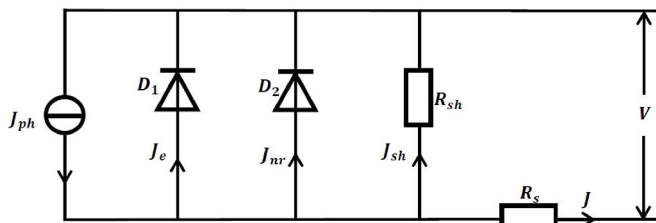


Fig. 1. The equivalent circuit model of perovskite solar cells.

J_e is the external radiative current density and defined as the photon flux that escapes the cell

$$J_e = J_0 \exp \left(\frac{q(V + JR_s)}{kT} \right) \quad (6)$$

where k is the Boltzmann constant, T is the Kelvin temperature, R_s is series resistance, J_0 is external radiative saturation current density and could be obtained in equation (10) by the black-body radiation law. Leakage current density through shunt resistors (R_{sh}) could be described as below

$$J_{sh} = \frac{V + JR_s}{R_{sh}} \quad (7)$$

According to blackbody radiation law, the blackbody formula is defined by [12].

$$\Phi(\lambda) = \frac{2hc^2}{\lambda^5} \frac{1}{\exp(hc/\lambda kT) - 1} \quad (8)$$

where the $\Phi(\lambda)$ is power emitted per area per wavelength per solid angle.

At thermal equilibrium states, the total photon emission rate for external solid angle Ω and polar angle θ can be obtained as equation (9)

$$\Gamma_0(\lambda) = \iint \Phi(\lambda) \cos \theta d\Omega = \int_0^{2\pi} d\phi \int_0^{\frac{\pi}{2}} \Phi(\lambda) \cos \theta \sin \theta d\theta = \pi \Phi(\lambda) \quad (9)$$

The reverse saturation current density in the thermal equilibrium situation can be written as below

$$J_0 = \frac{q}{hc} \int_{\lambda_{min}}^{\lambda_{max}} \lambda a(\lambda) \Gamma_0(\lambda) d\lambda \quad (10)$$

However, for practical solar cells, to derive the current in external circuit, in addition to radiative recombination, nonradiative recombination including Shockley-Read-Hall (SRH), surface and Auger recombination must be considered, which are given by these equations (11) ~ (14) [13, 21, 35].

$$R_{rad} = rnp = rn_i^2 \exp \left(\frac{q(V + JR_s)}{kT} \right) \quad (11)$$

$$R_{srh} = \frac{np - n_i^2}{n\tau_p - p\tau_n} = \frac{n_i}{2\tau_{srh}} \exp \left(\frac{q(V + JR_s)}{2kT} \right) \quad (12)$$

$$R_{surf} = \frac{np - n_i^2}{\frac{1}{S_p}(n + n_t) + \frac{1}{S_n}(p + p_t)} = \frac{n_i^2 S}{p_0^h} \exp \left(\frac{q(V + JR_s)}{kT} \right) + \frac{n_i^2 S}{n_0^e} \exp \left(\frac{q(V + JR_s)}{kT} \right) \quad (13)$$

$$R_{aug} = C_n n^2 p + C_p p^2 n = C_{aug} n_i^3 \exp \left(\frac{3q(V + JR_s)}{2kT} \right) \quad (14)$$

Where r is radiative recombination coefficient, τ_{srh} is SRH lifetime, S is surface recombination velocity, p_0^h/n_0^e is equilibrium hole/electron concentration near the perovskite side between perovskite layer and hole/electron transport layer interface, n_i is intrinsic carrier concentration with value of $2.3 \times 10^5 cm^{-3}$ [35], C_{aug} is Auger coefficient.

The recombination current density could be obtained by

$$J_R = q \int_0^L U dx = qUL \quad (15)$$

where L is the thickness of absorber layer and U is recombination rate per unit area. Thus, the recombination current density can be written as below

$$J_{rad} = qrn_i^2 L \exp\left(\frac{q(V + JR_s)}{kT}\right) \quad (16)$$

$$J_{srh} = \frac{qn_i}{2\tau_{srh}} L \exp\left(\frac{q(V + JR_s)}{2kT}\right) \quad (17)$$

$$J_{surf} = \frac{qn_i^2 S}{p_0^h} L_{surf} \exp\left(\frac{q(V + JR_s)}{kT}\right) + \frac{qn_i^2 S}{n_0^e} L_{surf} \exp\left(\frac{q(V + JR_s)}{kT}\right) \quad (18)$$

$$J_{aug} = qC_{aug} n_i^3 L \exp\left(\frac{3q(V + JR_s)}{2kT}\right) \quad (19)$$

where L_{surf} is the effective thickness of the interface between the transport layer and the active layer, the value of 0.02 nm is shown in Table 1.

2. Results

At a first step, one calculation is performed to identify the impact of the radiative and nonradiative recombination on the performance of perovskite solar cell as a function of cell thickness, assuming $R_{sh} \rightarrow \infty$ and $R_s = 0$.

2.1. Effect of radiative recombination

Fig. 2 shows a plot of the solar cell short circuit density (J_{sc}), open circuit voltage (V_{oc}), fill factor (FF) and power conversional efficiency (PCE) as a function of cell thickness under considering with and without photon recycling in absence of nonradiative recombination.

Considering photon recycling effect, the PCE increases with the thickness of the cell and reaches saturation when the thickness beyond 1 μm . Photon recycling has no essentially penalty on short circuit current, because light emission is quenched at short circuit by efficient charge carrier extraction, as seen in Fig. 2(a). The V_{oc} almost is independent of thickness due to constant external luminescence emission rate, which is in agreement with achieved results in Refs. [13,35].

However, in the absence of photon recycling effect, the V_{oc} degrades sharply and the FF also decreases slightly with increasing in cell thickness, resulting in a large drop in PCE with increased thickness. Therefore, photon recycling has very significant impact on V_{oc} of solar cell, thereby on PCE, which have been verified by several literatures [34–36].

2.2. Effect of SRH recombination

As mentioned above, the loss due to radiative recombination can be reduced by photon recycling, but non-radiative recombination will inevitably exist in realistic perovskite solar cells, yet what do they play roles on performance of perovskite solar cell? Firstly, one calculation is performed that the impact of SRH recombination on performance of perovskite solar cells. Fig. 3(a)(b)(c) shows V_{oc} , FF and PCE as a function of cell thickness with different SRH lifetime no considering other two recombination mechanisms (i.e., Auger and surface recombination). This representation yields the following results: (i) the SRH lifetime has significant impact on the performance of perovskite solar cells. The V_{oc} , FF and PCE drop with the reduction of SRH lifetime. (ii) the V_{oc} and FF are almost independent of the cell thickness when the thickness is lower than 1 μm and SRH lifetime beyond 100 μs . While the V_{oc} and FF will drop sharply when thickness is greater than 1 μm . (iii) the PCE enhances with increased thickness and reaches the maximum value at the cell thickness of around 0.5 μm , then drops with the further increase in cell thickness.

Table 1

The parameters of perovskite solar cells [13,28,35].

Parameter	τ_{srh} (μs)	S (cm^3/s)	C_{aug} (cm^6/s)	L_{surf} (nm)	n_0^e (cm^{-3})	p_0^h (cm^{-3})
Value	10	10^4	1×10^{-28}	0.02	9×10^{12}	9×10^{12}

The efficiency gains primarily come from continuous improvement in J_{sc} . (iv) to better understand the impact of SRH lifetime on the performance of thin film perovskite solar cells. Fig. 3(d) shows the performance of thin film perovskite solar cells with thickness of 500 nm as a function of SRH lifetime, the performance of solar cells drastically degrades as the SRH lifetime variation from 10 to 0.1 μs . For example, the PCE falls from approximate 28.5%–23%. The absolute efficiency drop is around 5.5% and the relative drop is 19.3%. But the performance almost has little changes with further increasing of the SRH lifetime from 10 to 100 μs , this is because radiative recombination dominates at high SRH lifetime.

2.3. Effect of surface recombination

Next, the impact of surface recombination on performance of perovskite solar cells is calculated. Fig. 4 shows the dependency of V_{oc} , FF and PCE on cell thickness with different surface recombination velocity (S), assuming in absence of other two non-radiative recombination mechanisms. It could be found from the plots: (i) the S almost does not impact the performances of perovskite solar cells when it is less than $10^3 cm/s$. While an increase in S from $S = 10^3$ to $S = 10^4 cm/s$ causes a large damage in performance, major penalty in the V_{oc} . (ii) the V_{oc} and FF are almost independent of cell thickness because S takes place at the interface between electron/hole transport layer and active layer. The PCE enhances with cell thickness and reaches saturation when the thickness is more than 1 μm due to improvement in J_{sc} with increased cell thickness. (iii) To better reveal the impact of S on the performance of a thin film perovskite solar cell, Fig. 4(d) shows the V_{oc} , PCE and FF as a function of S with cell thickness of 500 nm. Both V_{oc} and PCE reach saturation when the S is below $10^3 cm/s$, and the FF is nearly independent of S . Therefore, surface recombination does not appear to be an important limiting factor for further improving the efficiency of thin-film perovskite solar cells as long as it is below a certain value.

2.4. Effect of Auger recombination

Finally, the impact of Auger recombination as a function of cell thickness on the performance of cells will be calculated though this recombination mechanism has been certified by several literatures that it has slight impact on the performance of thin film perovskite solar cells [13,21,28,35]. Fig. 5 shows the V_{oc} , FF and PCE as a function of cell thickness with different Auger coefficient (C_{aug}), assuming no presence of other nonradiative recombination. On one hand, V_{oc} and PCE are almost independent of C_{aug} variation from 0.1×10^{-28} to $1 \times 10^{-28} cm^6/s$ when solar cell thickness is below 500 nm because radiative recombination is dominant. It should be noted that FF exhibits slight increase with increase in C_{aug} , as shown in Fig. 5(b). This can be explained by the fact that in decreasing the voltage from open-circuit to the maximum power operating point, the Auger recombination rate with higher C_{aug} drops faster than that with lower Auger coefficient, since Auger recombination rate is proportional to $C_{aug} \exp\left(\frac{3qV}{2kT}\right)$, as seen in equation (14). Therefore, the operating point voltage (V_{op}) in a cell with higher C_{aug} could be closer to the V_{oc} than in a cell with lower C_{aug} . To confirm our guess, Fig. 6 shows a plot of the difference between V_{oc} and V_{op} as a function of active layer thickness, which reveal that the $(V_{oc} - V_{op})$ gradually decreases with Auger coefficient variation from 0.1×10^{-28} to $100 \times 10^{-28} cm^6/s$, thereby increase in FF. A recent paper by Pazos-Onuton [41] has achieved similar results.

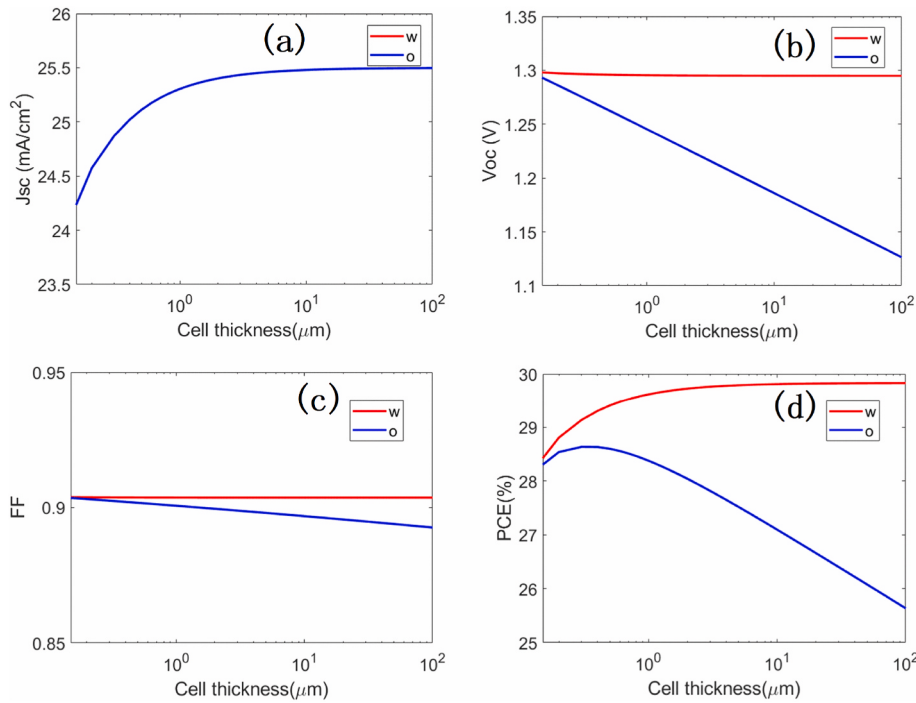


Fig. 2. (a) J_{sc} (b) V_{oc} (c) FF (d) PCE as a function of cell thickness with and without photon recycling. w: with photon recycling, o: without photon recycling.

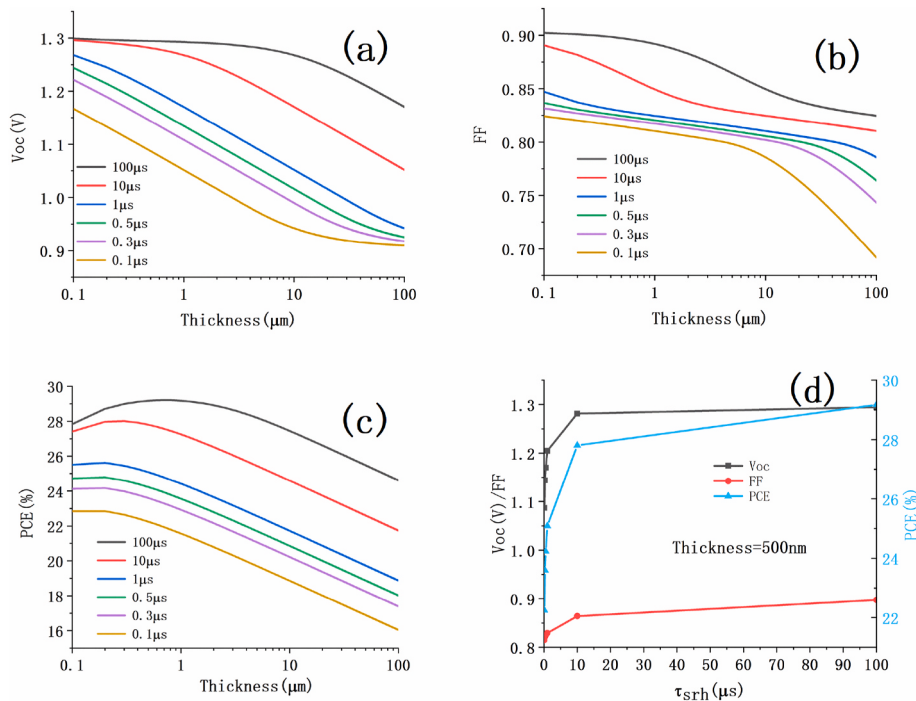


Fig. 3. (a) V_{oc} (b) FF (c) PCE as a function of thickness for different SRH lifetime. (d) the V_{oc} , FF and PCE of perovskite solar cell with a active layer thickness of 500 nm as a function of SRH lifetime.

Fig. 5(d) shows the performances of solar cells as a function of Auger recombination coefficient (C_{aug}) with cell thickness of 500 nm. An increase from $0.1 \times 10^{-28} \text{ cm}^6/\text{s}$ to $1 \times 10^{-28} \text{ cm}^6/\text{s}$ causes little damage, while a further increase causes a large drop in performance. In general, Auger coefficient for realistic perovskite solar is around $1 \times 10^{-28} \text{ cm}^6/\text{s}$ or less. Therefore, Auger recombination is not an important recombination mechanism for realistic perovskite solar cells, especially for thin film perovskite solar cells, which agree with achieved results in Refs.

[28,35].

2.5. Competition between radiative and nonradiative recombination

According to above simulation results, it could be found the nonradiative recombination has slight impact on performance of perovskite solar cells with thickness of less than 1 μm, and the PCE is closed to saturation when the cell thickness closed to 1 μm due to very high photon

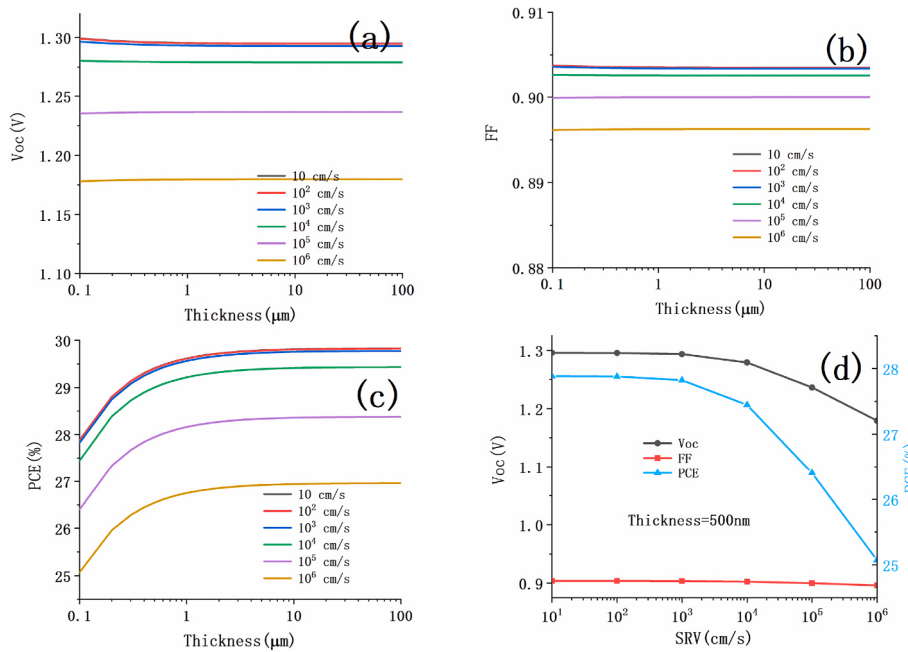


Fig. 4. (a) V_{oc} (b) FF (c) PCE as a function of thickness for different surface recombination velocity (S). (d) the V_{oc} , FF and PCE of a perovskite solar cell with the thickness of 500 nm as a function of surface recombination velocity (S).

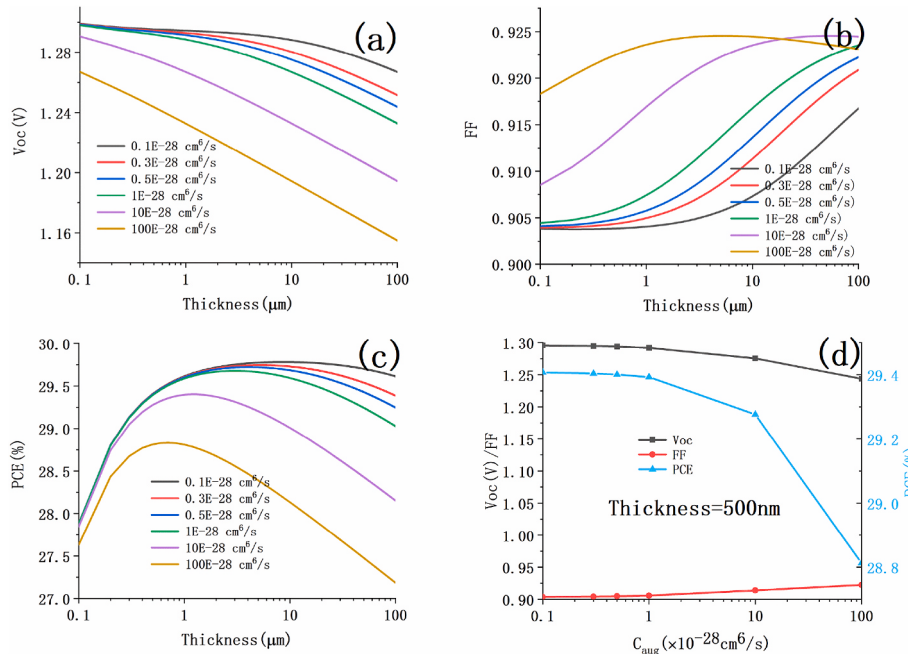


Fig. 5. (a) V_{oc} (b) FF (c) PCE as a function of thickness for Auger coefficient (C_{aug}). (d) the V_{oc} , FF and PCE of perovskite solar cell with the thickness of 500 nm as a function of Auger coefficient (C_{aug}).

absorbing coefficient. Therefore, in order to better demonstrate the recombination processes governing perovskite solar cells behavior for thin film perovskite solar cell, we calculate the J_{surf} , J_{rad} , $J_{e Aug}$ and J_{srh} as a function of voltage utilizing the SRH lifetime ($10 \mu\text{s}$) [28] and the Auger coefficients ($1 \times 10^{-28} \text{ cm}^6/\text{s}$) [35] as well as surface recombination velocity (10^4 cm/s) [13] reported, assuming cell thickness of 500 nm. The detailed parameters are summarized in Table 1.

Fig. 7(a) shows the individual recombination component as a function of voltage. Each component is achieved using (6), (15), (16), (17) and (18), respectively. Fig. 7(b) shows the fraction of each

recombination current, which is its individual recombination current divided by the total recombination current. SRH recombination is dominant and internal radiative recombination is subdominant at operating point, which is responsible for $\sim 65.5\%$ and $\sim 22.5\%$ of total recombination, respectively. The remainder is mainly from surface recombination and external radiative recombination, and accounts for 6% , respectively. Auger recombination is an inevitable loss mechanism in perovskite solar cells, but has almost negligible effect on cell performance at the operating point, as seen in Fig. 7(b). This is due to lower carrier concentration in active layer at the operating voltage leading to low Auger recombination rate. The orange dotted line in Fig. 7(b) is the

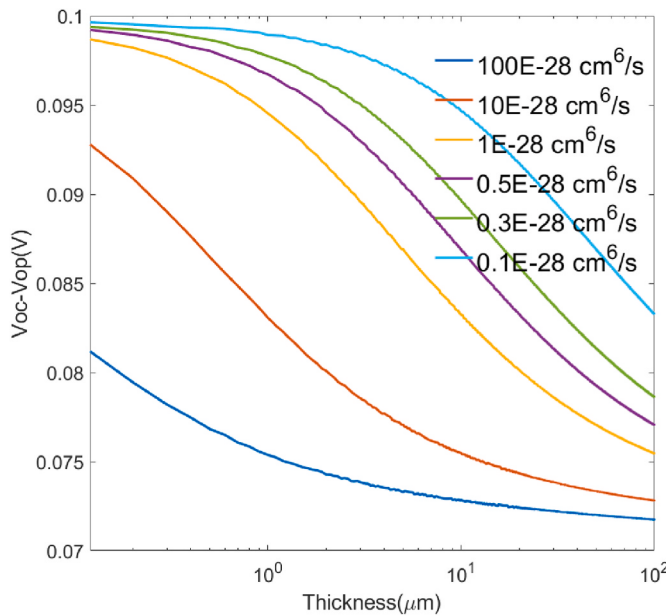


Fig. 6. The difference between V_{oc} and V_{op} as a function of active layer thickness.

voltage corresponding to the operating point.

2.6. Effects of series and shunt resistance

Previous literatures [42] have demonstrated series and shunt resistance can result in significant loss in efficiency due to lowering the FF. In this paper, Fig. 8(a) and (b) show the impact on performance of solar cells due to different series and shunt resistance values, respectively. FF and PCE appear to degrade with increasing series resistance or decreasing shunt resistance values, while J_{sc} and V_{oc} are independent of them, which are in agreement with reference [42].

Series resistance has a significant effect on performance of solar cells, and PCE appears to decrease almost linearly with increasing series resistance. But the effect of shunt resistance on performance is nearly negligible when the shunt resistance is greater than $10^4 \Omega \cdot \text{cm}^2$.

2.7. Breakdown of loss mechanisms

Fig. 9 shows a detailed illustration of the PCE drop introduced by different loss factors in different orders, showing how much PCE is dropped by each loss factor and serving to identify the most critical loss factors. Auger recombination is much less significant, the overall PCE is slightly degraded from SQ limit to Auger loss. PCE suffers significantly (to 28.99%) due to lowering V_{oc} from Auger loss to surf loss. SRH recombination further lowers the efficiency (to 27.72%) by reducing V_{oc}

from surf loss to SRH loss. Finally, a $0.6 \Omega \cdot \text{cm}^2$ series resistance (R_s) and $10^4 \Omega \cdot \text{cm}^2$ shunt resistance (R_{sh}) cause further drop in efficiency to 27.37% from SRH loss to R_s loss and 27.24% from R_s loss to R_{sh} loss, respectively.

3. Discussion

We have investigated the impacts of various loss mechanisms, including radiative and non-radiative as well as ohmic loss, on the performances of perovskite solar cells. As perovskite solar cells conversion efficiency is constantly improving, it is much necessary to clarify the key loss factors impacting the perovskite solar cells conversion efficiency in order to obtain the pathway of solar cells closed to limit efficiency. Because not each loss mechanism affects conversion efficiency equally. For example, in this paper, the achieved results shows that Auger recombination is very low and has negligible effect on the PCE. Further lowering the surface recombination velocity of below 10^4 cm/s or optimization of shunt resistance of more than $10^4 \Omega \cdot \text{cm}^2$, would not increase the efficiency significantly. However, improvements in SRH life-time from $1\mu\text{s}$ to $10\mu\text{s}$ will increase around 3% in absolute efficiency significantly (see Fig. 3), and further improvement to $100\mu\text{s}$ leading to further increase of around 1% in efficiency. Generally, the SRH lifetime is on the range of $0.001\text{--}10\mu\text{s}$ [27]. Therefore, the SRH lifetime is one of the most important loss mechanisms for limiting conversion efficiency in perovskite solar cells, which can be explained by equation (20), [43]. Because V_{oc} will be penalized due to poor external luminescence efficiency (η_{ext}).

$$V_{oc} = V_{oc-max} - \left| \frac{kT}{q} \ln (\eta_{ext}) \right| \quad (20)$$

where η_{ext} is the external radiative recombination divided by total recombination (including radiative and non-radiative recombination) at V_{oc} . It is obvious that poor η_{ext} leads to drop in V_{oc} logarithmically when SRH loss dominates in all loss mechanisms.

Besides SRH recombination, another most important factor affecting efficiency is series resistance, as efficiency nearly decreases linearly with increasing series resistance, as seen in Fig. 7(c).

Comparing with previous literatures [34–37], the similar results are achieved on the impact of radiative, SRH and Auger recombination on the performance. Unfortunately, previous studies did not involve surface recombination and ohmic loss. In this paper, we comprehensively numerically simulate the impact of loss mechanisms on the impact of perovskite solar cells.

As a final remark, there are several approaches to mitigating SRH and surface recombination, such as the control of perovskite crystallization [44,45], defect passivation [46,47] and interface engineering [48–51] and so on. Among of them, controlling crystallization is the most effective means to achieve high quality perovskite film. SRH recombination dominates the non-radiative recombination losses in a complete perovskite solar cell. A recent study has shown one could use

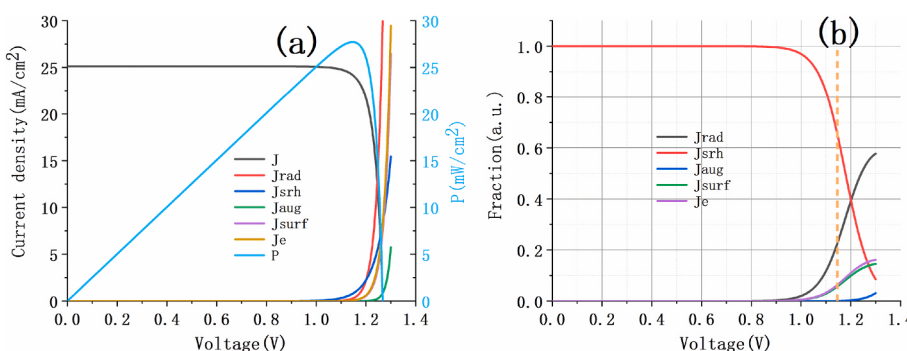


Fig. 7. (a) Simulated P – V and J – V curves are shown with the magnitude of SRH, radiative, external radiative, surface and Auger recombination current density as a function of voltage. (b) The fractions of total recombination current due to SRH, radiative, external radiative, surface and Auger recombination are shown at each voltage. The orange dotted line denotes the voltage corresponding to the maximum power. (For interpretation of the references to colour in this figure legend, the reader is referred to the Web version of this article.)

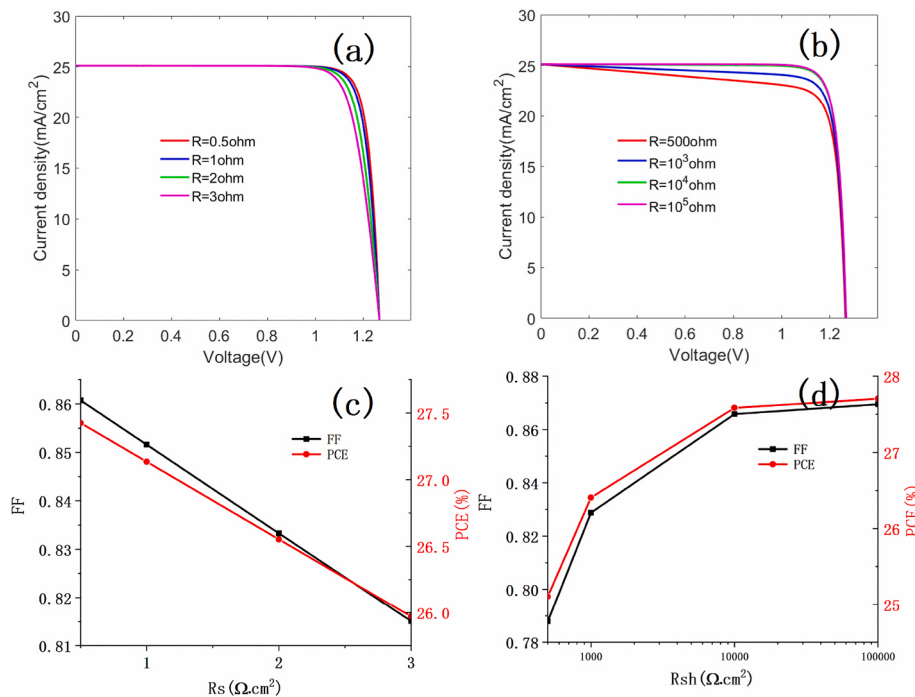


Fig. 8. The impact of series resistance (a)(c) and shunt resistance(b)(d) on the performance of perovskite solar cells.

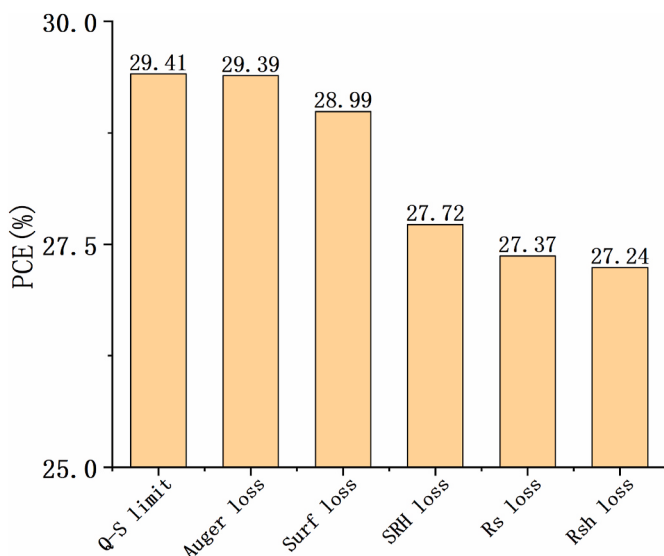


Fig. 9. List of loss mechanisms considered and their impacts on cell efficiency.

the organic molecules with specific functional groups or govern the strength of the hydrogen bonds between the passivation functional groups and the perovskite to passivate these defects, thereby improving the SRH carrier lifetime [52]. Inserting an ultrathin ferroelectric polymer layer at the perovskite/top-extraction layer interface, one can obtain a favorable energy-level alignment, thereby minimizing interface-induced recombination losses [53]. In addition, molecular modifiers (e.g., tri-n-octylphosphine oxide, TOPO) are also often applied to passivate the surface traps. Braly et al. [54] recently demonstrated that a surface recombination velocity of less than 10^3 cm/s is achieved after passivating the top surface with TOPO.

4. Conclusion

In this paper, we numerically investigate the loss factors limiting the performance of perovskite solar cells, our purpose is to identify the dominant loss factors by comprehensively studying various loss mechanism playing roles on the performances of perovskite solar cells. The achieved results demonstrate SRH recombination and series resistance is the most important two of factors limiting the performances of devices. The PCE nearly drops linearly with the reduction of lifetime when lifetime is less than $1 \mu\text{s}$. The PCE drops approximate 5% point as the lifetime varies from 1 to $0.1 \mu\text{s}$ for cells with 500 nm in thickness. Meanwhile, similar to SRH, the PCE also nearly reduces linearly with the series resistance increasing from 0.1 to 3Ω , and absolute drop efficiency of 1.5% point. On the other hand, the perovskite solar cell in efficiency also suffers from surface recombination significantly, but the performance is almost independent of surface recombination velocity when the surface recombination velocity is lower than 10^4 cm/s . Auger recombination is very low and has no significant impact on the device performance. The effect of the shunt resistance on performance is nearly negligible when the shunt resistance is greater than $10^4 \Omega \cdot \text{cm}^2$. Therefore, it is concluded that SRH recombination and series resistance is the most important two of factors limiting the performance of perovskite solar cell. It is necessary to develop technologies to achieve very high SRH lifetime and very low series resistance to approach the ultimate efficiency limit of perovskite solar cells.

Credit author statement

Yinsheng Peng: Formal analysis, Writing-Original draft; Shurong Wang: Data curation, Funding acquisition and Conceptualization. Long Li and Zhineng Zhou: Software, Zuming Liu: Writing-Reviewing and Editing, Shouli Zhou: Validation, Minghai Yao: Funding acquisition.

Declaration of competing interest

The authors declare that they have no known competing financial interests or personal relationships that could have appeared to influence the work reported in this paper.

Data availability

Data will be made available on request.

Acknowledgements

The authors would like to thank National Nature Science Foundation of China (Grant Nos. 61871350 and U1902218) for their financial support of this research.

References

- [1] C. Wehrenfennig, G.E. Eperon, M.B. Johnston, H.J. Snaith, L.M. Herz, High charge carrier mobilities and lifetimes in organolead trihalide perovskites, *Adv. Mater.* 26 (2014) 1584–1589.
- [2] S.D. Stranks, G.E. Eperon, G. Grancini, C. Menelaou, M.J.P. Alcocer, T. Leijtens, L. M. Herz, A. Petrozza, H.J. Snaith, Electron-hole diffusion lengths exceeding 1 micrometer in an organometal trihalide perovskite absorber, *Science* 342 (2013) 341–344.
- [3] D. Bi, W. Tress, M.I. Dar, P. Gao, J. Luo, C.m. Renier, K. Schenck, A. Abate, F. Giordano, J.P. Correa Baena, et al., Efficient luminescent solar cells based on tailored mixed-cation perovskites, *Sci. Adv.* 2 (2016), e1501170.
- [4] D.W. deQuilettes, S.M. Vorpahl, S.D. Stranks, H. Nagaoka, G.E. Eperon, M.E. Ziffer, H.J. Snaith, D.S. Ginger, Impact of microstructure on local carrier lifetime in perovskite solar cells, *Science* 348 (2015) 683–686.
- [5] D.W. deQuilettes, W. Zhang, V.M. Burlakov, D.J. Graham, T. Leijtens, A. Oshero, V. Bulovic, H.J. Snaith, D.S. Ginger, S.D. Stranks, Photo-induced halide redistribution in organic-inorganic perovskite films, *Nat. Commun.* 7 (2016), 11683.
- [6] M.A. Green, A.H. Baillie, H.J. Snaith, Perovskite solar cells with a planar heterojunction structure prepared using room-temperature solution processing techniques, *Nat. Photonics* 8 (2014) 133–138.
- [7] H.S. Kim, C.R. Lee, J.H. Im, K.B. Lee, T. Moehl, A. Mar-choro, S.J. Moon, R. H. Baker, J.H. Yum, J.E. Moser, M. Grätzel, N.G. Park, Lead iodide perovskite sensitized all-olid-statesubmicron thin film mesoscopic solar cell with efficiency exceeding 9%, *Sci. Rep.* 2 (2012) 591.
- [8] J. Burschka, N. Pellet, S.J. Moon, R.H. Baker, P. Gao, M.K. Nazeeruddin, M. Grätzel, Sequential deposition as a route to high-performance perovskite-sensitized solar cells, *Nature* 499 (2013) 316–319.
- [9] M.Z. Liu, M.B. Johnston, H.J. Snaith, Efficient planar heterojunction perovskite solar cells by vapour deposition, *Nature* 501 (2013) 395–398.
- [10] M. Liu, M.B. Johnston, H.J. Snaith, Efficient planar heterojunction perovskite solar cells by vapour deposition, *Nature* 501 (2013) 395–398.
- [11] A. Martin, Green, ewan D. Dunlop, jochen hohlf-ebinger, masahiro yoshita, nikos Kopidakis, Xiaoqing hao, solar cell efficiency tables (version 58), *Prog. Photovoltaics Res. Appl.* 29 (2021) 657–667.
- [12] Wei E.I. Sha, Xingang Ren, Luzhou Chen, Wallace C.H. Choy, The efficiency limit of CH₃NH₃PbI₃ perovskite solar cells, *Appl. Phys. Lett.* 106 (22) (2015) 221104. Jun.
- [13] Ting Xu, Zi-Shuai Wang, Li Xuan-Hua, E.I. Sha Wei, Loss mechanism analyses of perovskite solar cells with equivalent circuit model, *Acta Phys. Sin.* 70 (No. 9) (2021), 098801.
- [14] W. Shockley, H.J. Queisser, Detailed balance limit of efficiency of pn-junction solar cells, *J. Appl. Phys.* 32 (1961) 510–519.
- [15] W. van Roosbroeck, W. Shockley, Photon-radiative recombination of electrons and holes in Germanium, *Phys. Rev.* 94 (1954) 1558–1560.
- [16] Xufeng Wang, Student Member, , IEEE, Mohammad Ryyan Khan, Jeffery L. Gray, Design of GaAs solar cells operating close to the shockley-queisser limit, *IEEE J. Photovoltaics* 3 (NO. 2) (APRIL 2013).
- [17] L.M. Pazos-Outon, M. Szumilo, R. Lamboll, J.M. Richter, M. Crespo-Quesada, M. Abdi-Jalebi, H.J. Beeson, M. Vrucinic, M. Alsari, H.J. Snaith, et al., Photon recycling in lead iodide perovskite solar cells, *Science* 351 (2016) 1430–1433.
- [18] M. Saliba, W. Zhang, V.M. Burlakov, S.D. Stranks, Y. Sun, J.M. Ball, M.B. Johnston, A. Goriely, U. Wiesner, H.J. Snaith, Plasmonic-induced photon recycling in metal halide perovskite solar cells, *Adv. Funct. Mater.* 25 (2015) 5038–5046.
- [19] M.A. Steiner, J.F. Geisz, I. García, D.J. Friedman, A. Duda, S.R. Kurtz, Optical enhancement of the open circuit voltage in high quality GaAs solar cells, *J. Appl. Phys.* 113 (2013), 123109.
- [20] R.K. Ahrenkiel, D.J. Dunlavay, B. Keyes, S.M. Vernon, T.M. Dixon, S.P. Tobin, K. L. Miller, R.E. Hayes, Ultralong minority-carrier lifetime epitaxial GaAs by photon recycling, *Appl. Phys. Lett.* 55 (1989) 1088.
- [21] A.W. Walker, O. Höhn, D.N. Micha, B. Bläsi, A.W. Bett, F. Dimroth, Impact of photon recycling on GaAs solar cell designs, *IEEE J. Photovoltaics* 5 (2015) 1636.
- [22] A. Braun, E.A. Katz, D. Feuermann, B.M. Kayes, J.M. Gordon, Photovoltaic performance enhancement by external recycling of photon emission, *Energy Environ. Sci.* 6 (2013) 1499.
- [23] L.M. Pazos-Outon, M. Szumilo, R. Lamboll, J.M. Richter, M. Crespo-Quesada, M. Abdi-Jalebi, H.J. Beeson, M. Vru ini, M. Alsari, H.J. Snaith, B. Ehrler, R. H. Friend, F. Deschler, Photon recycling in lead iodide perovskite solar cells, *Science* 351 (2016) 1430.
- [24] Y. Fang, H. Wei, Q. Dong, J. Huang, Quantification of re-absorption and re-emission processes to determine photon recycling efficiency in perovskite single crystals, *Nat. Commun.* 8 (2017), 14417.
- [25] W. Tress, Perovskite solar cells on the way to their radiative efficiency limit – insights into a success story open-circuit voltage and low recombination, *Adv. Energy Mater.* 7 (2017), 1602358.
- [26] J.M. Richter, M. Abdi-Jalebi, A. Sadhanala, M. Tabachnyk, J.P.H. Rivett, L. M. Pazos-Outón, K.C. Gödel, M. Price, F. Deschler, R.H. Friend, Enhancing photoluminescence yields in lead halide perovskites by photon recycling and light out-coupling, *Nat. Commun.* 7 (2016), 13941.
- [27] M.B. Johnston, L.M. Herz, Hybrid perovskites for photovoltaics: charge-carrier recombination, diffusion, and radiative efficiencies, *Acc. Chem. Res.* 49 (2016) 146.
- [28] I. Braly, D.W. deQuilettes, L.M. Pazos-Outón, S. Burke, M.E. Ziffer, D.S. Ginger, H. W. Hillhouse, Hybrid perovskite films approaching the radiative limit with over 90% internal photoluminescence quantum efficiency, *Nat. Photonics* 12 (2018) 355.
- [29] Q. Dong, Y. Fang, Y. Shao, P. Mulligan, J. Qiu, L. Cao, J. Huang, Electron-hole diffusion lengths > 175 μm in solution-grown CH₃NH₃PbI₃ single crystals, *Science* 347 (2015) 967.
- [30] Y. Fang, Q. Dong, Y. Shao, Y. Yuan, J. Huang, Highly narrowband perovskite single-crystal photodetectors enabled by surface-charge recombination, *Nat. Photonics* 9 (2015) 679.
- [31] Y. Yamada, T. Yamada, Y. Kanemitsu, Free carrier radiative recombination and photon recycling in lead halide perovskite solar cell materials, *Bull. Chem. Soc. Jpn.* 90 (2017) 1129.
- [32] T. Yamada, Y. Yamada, Y. Nakaike, A. Wakamiya, Y. Kanemitsu, Photon emission and reabsorption processes in CH₃NH₃PbBr₃ single crystals revealed by time-resolved two-photon-excitation photoluminescence microscopy, *Phys. Rev. Appl.* 7 (2017), 014001.
- [33] Y. Kanemitsu, Luminescence spectroscopy of lead-halide perovskites: materials properties and application as photovoltaic devices, *J. Mater. Chem. C* 5 (2017) 3427.
- [34] Thomas Kirchartz, Florian Staub, Uwe Rau, Impact of photon-recycling on the open-circuit voltage of metal halide perovskite solar cells, *ACS Energy Lett.* (2016), 07 Sep.
- [35] Roberto Brenes, Madeleine Laitz, Joel Jean, W. Dane, deQuilettes, and vladimir Bulovic', benefit from photon recycling at the maximum-power point of state-of-the-art perovskite solar cells, *PHYSICAL REVIEW APPLIED* 12 (2019), 014017.
- [36] I. Braly, D.W. deQuilettes, L.M. Pazos-Outón, S. Burke, M.E. Ziffer, D.S. Ginger, H. W. Hillhouse, Hybrid perovskite films approaching the radiative limit with over 90% internal photoluminescence quantum efficiency, *Nat. Photonics* 12 (2018) 355.
- [37] L.M. Pazos-Outón, T.P. Xiao, E. Yablonovitch, Fundamental efficiency limit of lead iodide perovskite solar cells, *J. Phys. Chem. Lett.* 9 (2018) 1703.
- [38] T. Tieged, E. Yablonovitch, G.D. Cody, B.G. Brooks, Limiting efficiency of silicon solar cells, *IEEE Trans. Electron. Dev.* 31 (5) (1984) 711–716.
- [39] E. Yablonovitch, Statistical ray optics, *J. Opt. Soc. Am.* 72 (1982) 889–907. Jul.
- [40] Philipp López, Michael Stuckelberger, Björn Niesen, Jérémie Werner, Miha Filipić, SooJin Moon, Jun-Ho Yum, Marko Topic, Stefaan De Wolf, Christophe Ballif, Complex refractive index spectra of CH₃NH₃PbI₃ perovskite thin films determined by spectroscopic ellipsometry and spectrophotometry, *J. Phys. Chem. Lett.* 6 (2015) 1.
- [41] Pazos-Outon, LM; Xiao, TP and Yablonovitch, E, Fundamental efficiency limit of lead iodide perovskite solar cells, *J. Phys. Chem. Lett.* 9 (7) , pp.1703-1711.
- [42] M.A. Green, K. Emery, Y. Hishikawa, W. Warta, E.D. Dunlop, Solar cell efficiency tables (Version 39), *Prog. Photovoltaics* 20 (1) (2012) 12–20.
- [43] Owen D. Miller, Eli Yablonovitch, Sarah R. Kurtz, Strong internal and external luminescence as solar cells approach the shockley-queisser limit, *IEEE J. Photovoltaics* 2 (NO. 3) (2012). JULY.
- [44] M. Abdi-Jalebi, et al., Maximizing and stabilizing luminescence from halide perovskites with potassium passivation, *Nature* 555 (2018) 497–501.
- [45] M. Saliba, et al., Incorporation of rubidium cations into perovskite solar cells improves photovoltaic performance, *Science* 354 (2016) 206–209.
- [46] Y. Shao, Z. Xiao, C. Bi, Y. Yuan, J. Huang, Origin and elimination of photocurrent hysteresis by fullerene passivation in CH₃NH₃PbI₃ planar heterojunction solar cells, *Nat. Commun.* 5 (2014) 5784.
- [47] S. Yang, et al., Tailoring passivation molecular structures for extremely small open-circuit voltage loss in perovskite solar cells, *J. Am. Chem. Soc.* 141 (2019) 5781–5787.
- [48] Q. Wang, Q. Dong, T. Li, A. Gruverman, J. Huang, Thin insulating tunneling contacts for efficient and water-resistant perovskite solar cells, *Adv. Mater.* 28 (2016) 6734–6739.
- [49] Y. Shao, Y. Yuan, J. Huang, Correlation of energy disorder and open-circuit voltage in hybrid perovskite solar cells, *Nat. Energy* 1 (2016), 15001.
- [50] Q. Jiang, et al., Surface passivation of perovskite film for efficient solar cells, *Nat. Photonics* 13 (2019) 460–466.
- [51] X. Zheng, et al., Defect passivation in hybrid perovskite solar cells using quaternary ammonium halide anions and cations, *Nat. Energy* 2 (2017), 17102.
- [52] W. Xu, et al., Rational molecular passivation for high-performance perovskite light-emitting diodes, *Nat. Photonics* 13 (2019) 418–424.
- [53] C.C. Zhang, et al., Polarized ferroelectric polymers for high-performance perovskite solar cells, *Adv. Mater.* 31 (2019), 1902222.
- [54] I.L. Braly, D.W. DeQuilettes, L.M. Pazos-Outón, S. Burke, M.E. Ziffer, D.S. Ginger, H.W. Hillhouse, Hybrid perovskite films approaching the radiative limit with over 90% photoluminescence quantum efficiency, *Nat. Photonics* 12 (2018) 355.